ADVANCED HEALTHCARE MATERIALS
www.advhealthmat.de

Photocrosslinkable Gelatin Hydrogel for Epidermal Tissue Engineering

*Xin Zhao, Qi Lang, Lara Yildirimer, Zhi Yuan Lin, Wenguo Cui, Nasim Annabi, Kee Woei Ng, Mehmet R. Dokmeci, Amir M. Ghaemmaghami, and Ali Khademhosseini**

Natural hydrogels are promising scaffolds to engineer epidermis. Currently, natural hydrogels used to support epidermal regeneration are mainly collagen- or gelatin-based, which mimic the natural dermal extracellular matrix but often suffer from insufficient and uncontrollable mechanical and degradation properties. In this study, a photocrosslinkable gelatin (i.e., gelatin methacrylamide (GelMA)) with tunable mechanical, degradation, and biological properties is used to engineer the epidermis for skin tissue engineering applications. The results reveal that the mechanical and degradation properties of the developed hydrogels can be readily modified by varying the hydrogel concentration, with elastic and compressive moduli tuned from a few kPa to a few hundred kPa, and the degradation times varied from a few days to several months. Additionally, hydrogels of all concentrations displayed excellent cell viability (>90%) with increasing cell adhesion and proliferation corresponding to increases in hydrogel concentrations. Furthermore, the hydrogels are found to support keratinocyte growth, differentiation, and stratification into a reconstructed multilayered epidermis with adequate barrier functions. The robust and tunable properties of GelMA hydrogels suggest that the keratinocyte laden hydrogels can be used as epidermal substitutes, wound dressings, or substrates to construct various in vitro skin models.

1. Introduction

Healing of cutaneous wounds involves regeneration of surface epidermis and repair of connective tissues. Re-epithelialization precedes repair in the dermis and accelerates the process of wound healing.[1,2] It also provides early re-establishment of a functional barrier, which is vital in the prevention of excessive transepidermal water loss and infection.[3] Therefore, re-epithelialization is considered a primary step in cutaneous wound healing.[2]

Various types of tissue engineered scaffolds have been developed and used for engineering epidermis.[4] Ideally, these scaffolds should exhibit certain biological features (i.e., to support keratinocyte adhesion, proliferation, and differentiation) and possess appropriate mechanical and degradation properties.[5] Mechanical properties of the scaffolds have been identified as a key modulator in keratinocyte behavior

Dr. X. Zhao, Q. Lang, Dr. L. Yildirimer, Z. Y. Lin, Prof. N. Annabi, Dr. M. R. Dokmeci, Prof. A. Khademhosseini
Biomaterials Innovation Research Center
Division of Biomedical Engineering
Department of Medicine
Brigham and Women's Hospital
Harvard Medical School
Boston 02139, MA, USA
E-mail: alik@rics.bwh.harvard.edu

Dr. X. Zhao, Q. Lang, Dr. L. Yildirimer, Z. Y. Lin, Prof. N. Annabi, Dr. M. R. Dokmeci, Prof. A. Khademhosseini
Harvard-MIT Division of Health Sciences and Technology
Massachusetts Institute of Technology
Cambridge 02139, MA, USA

Dr X. Zhao, Prof. A. M. Ghaemmaghami
Division of Immunology
School of Life Sciences
Faculty of Medicine and Health Sciences
Queen's Medical Centre
University of Nottingham
Nottingham NG7 2UH, UK

Prof. W. Cui
Orthopedic Institute
Soochow University
708 Renmin Rd, Suzhou, Jiangsu 215006, China

Dr. N. Annabi, Dr. M. R. Dokmeci, Prof. A. Khademhosseini
Wyss Institute for Biologically Inspired Engineering
Harvard University
Boston 02115, MA, USA

Prof. K. W. Ng
School of Materials Science and Engineering
Nanyang Technological University
N4.1 50 Nanyang Avenue, Singapore 639798, Singapore

Prof. A. Khademhosseini
Department of Physics
King Abdulaziz University
Jeddah 21569, Saudi Arabia

DOI: 10.1002/adhm.201500005

with increased cell adhesion and proliferation on stiffer substrates with compressive moduli of around 100 kPa.[6] The scaffolds should also be sufficiently strong and elastic for facile handling during surgery[7] and for supporting natural movements of the tissues.[8] Additionally, such scaffolds should ideally degrade only after adequate healing, which could take more than 8 weeks.[9] Furthermore, for some clinical applications, the scaffolds are required to be rapidly crosslinked in situ, allowing for optimal molding toward the wound contour.[10]

Based on these requirements, natural hydrogels are considered as attractive candidates to engineer epidermis due to their unique combination of biological and physical properties including biocompatibility as they mimic extracellular matrix (ECM), adjustable mechanical, swelling and degradation properties, as well as in situ crosslinking capabilities.[11,12] Amongst natural hydrogels, collagen is highly popular as collagen is the major component of the basement membrane on which the epidermis sits, thereby supporting keratinocyte proliferation, migration, and differentiation.[13,14] However, some of the limitations of collagen hydrogels for epidermis regeneration include their low mechanical properties and fast degradation rate.[15] These challenges could be tackled by varying collagen concentrations (which may lead to heterogeneity of hydrogels)[16,17] or by plastic compression (which needs postprocessing of hydrogels).[18,19] Additionally, higher mechanical strength and slower degradation rates could be achieved at the expense of elasticity as demonstrated by Awang et al. resulting in a stronger but brittle scaffold.[20] Other weaknesses of collagen include potential toxicities caused by chemical cross-linking agents (e.g., glutaraldehyde) that are generally employed to improve mechanical properties and stability.[21] Therefore, currently developed collagen hydrogels remain suboptimal as scaffolds for skin substitutes.

As an alternative to collagen, gelatin (i.e., hydrolyzed collagen) has attracted increasing attention as it has relatively low antigenicity compared to collagen whilst maintaining the properties of biocompatibility and biodegradability, in addition to being significantly less expensive than collagen.[21] Modification of gelatin with photocrosslinkable methacrylamide groups (GelMA) maintains the unique properties of gelatin, but additionally endows the material to be solidified from liquid to solid permanently via chemical reaction of the methacrylamide groups.[22] The hydrogel prepolymer solution can be spread on the wound area of different shapes and rapidly crosslinked in situ toward the wound contour upon light exposure. By selecting proper photoinitiators (PIs, e.g., Irgacure 2959), high crosslinking degree of polymer can be achieved within minutes or even seconds at low concentration of PIs, minimizing cytotoxicity.[23] In addition, the transparent nature of crosslinked GelMA allows for easy observation of cellular behavior encapsulated within or seeded onto the hydrogel. Furthermore, by varying the methacrylamide modification degree, GelMA concentration, or photopolymerization time (i.e., to change the polymer crosslinking density for controlling the hydrogel network structure), its mechanical, degradation, and biological properties can be easily tuned.[22,24] Such control of the hydrogel network structure endows the scaffolds with the proper design characteristics of the physical and biological properties. Hence, the mechanical, degradation, and biological properties of the GelMA hydrogels can be varied in a controlled manner and with relative ease to allow for applications as skin substitutes at different body sites and for different wound types. Application of GelMA hydrogels in tissue engineering (e.g., blood vessel regeneration) has been published previously.[22,24] The present study focuses on a novel application of GelMA hydrogels in skin regeneration, which needs stiffer and stronger surfaces to support keratinocyte adhesion and proliferation[6] and significant prolonged degradation profiles as cutaneous wounds frequently heal over longer periods of time of up to 8 weeks.[9]

In this paper, GelMA hydrogels with varying concentrations were synthesized for epidermal reconstruction. The physical properties of the hydrogels were fine-tuned by systematically varying GelMA concentrations to control keratinocyte adhesion, proliferation, and differentiation. Finally, a confluent keratinocyte monolayer was developed and reconstruction of stratified and functional epidermis was achieved using the hydrogel scaffolds.

2. Results and Discussion

2.1. Physical Properties of GelMA Hydrogels

The synthesized GelMA was found to have a degree of methacrylamide modification of 75%, consistent with previous reports (data not shown).[25] Upon UV exposure, the prepolymer solution of GelMA could form a crosslinked network (Figure S1A, Supporting Information). It was found that at all concentrations of GelMA ranging from 5% to 20%, the gel precursor solution could be injected via a conventional 27-gauge needle into a PDMS mold to form hydrogels of various shapes (round, square, star, and triangle) after UV polymerization (Figure S1B, Supporting Information).

First, we characterized the scaffold's mechanical properties as these are important parameters for engineering optimal skin substitutes. Compressive stress–strain curves illustrated a positive correlation between GelMA concentrations and compressive moduli, ranging from less than 5 kPa (5% GelMA) to ≈110 kPa (20% GelMA) ($p < 0.05$, **Figure 1**A,B), likely due to an increased crosslinking density at higher GelMA concentrations. High compressive moduli (≈100 kPa) have previously been demonstrated to be favorable for keratinocyte growth.[6]

Tensile stress–strain curves followed a similar trend with increasing GelMA concentrations resulting in higher elastic moduli and ultimate strength ($p < 0.05$) (Figure 1C). 20% GelMA hydrogels were found to have elastic moduli of up to 200 kPa and ultimate strengths of 30 kPa. Such high values are beneficial considering the significant amount of stretching and bending forces exerted during wound healing.[26] Although higher GelMA concentrations correlated with reduced elongation at break points from 40% (5% GelMA) to 20% (20% GelMA) possibly due to the increased crosslinking density limiting hydrogel deformation, the 20% extensibility may still be considered appropriate for skin substitutes.[8] In summary, robust yet tunable mechanical properties of GelMA hydrogels make them ideal candidates as substitute materials for skin regeneration as their properties can mirror the broad range of elasticity found in native skin.[8]

Adv. Healthcare Mater. 2015,
DOI: 10.1002/adhm.201500005

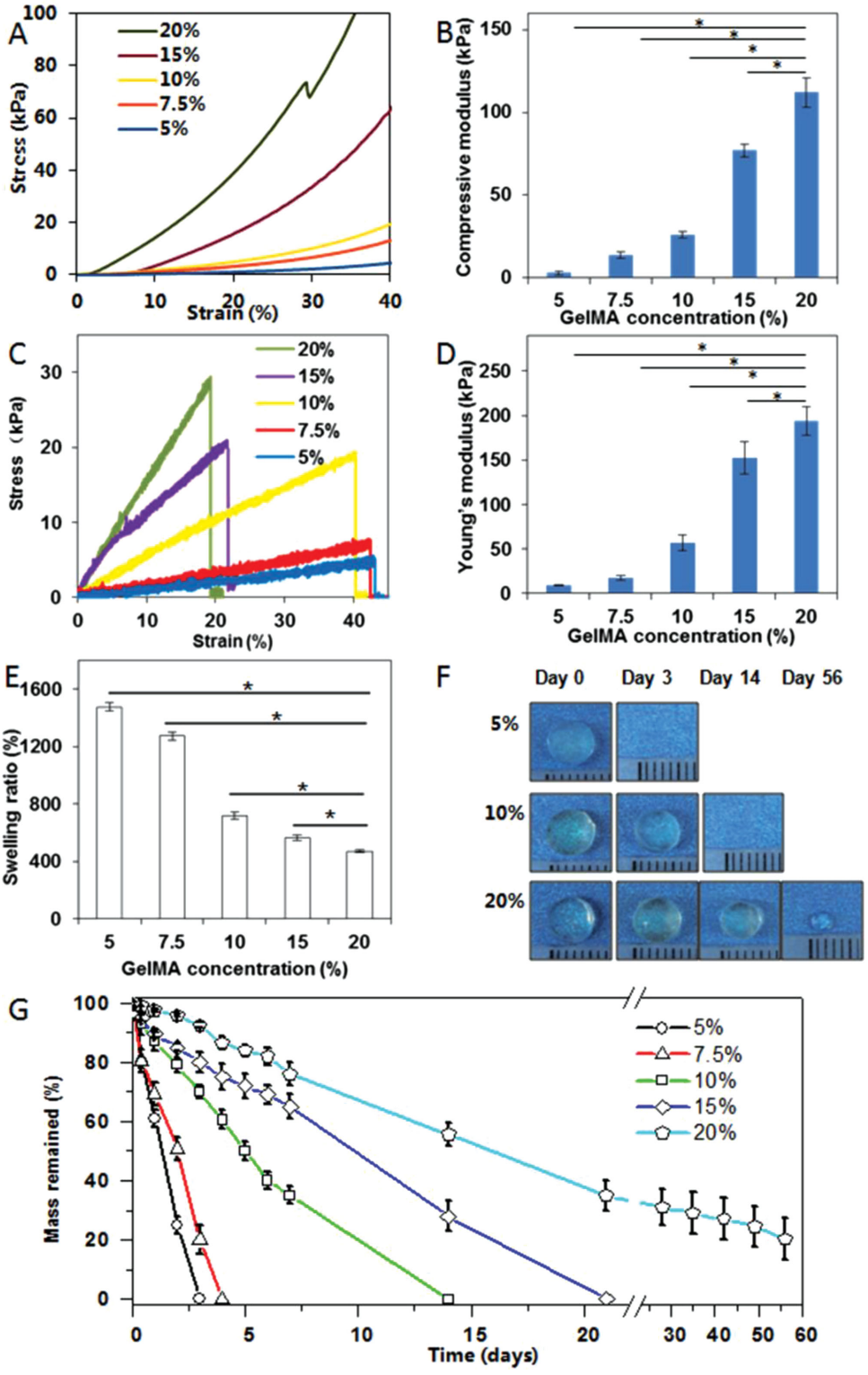

Figure 1. A) Compressive stress–strain characterization, B) compressive modulus, C) tensile stress–strain curves, D) tensile modulus, E) swelling ratio, F) representative photographs of morphology changes during in vitro degradation, and G) mass retention during degradation of GelMA hydrogels of varying concentrations. Note that about 25% of 20% GelMA remained after 56 d of degradation study. * indicates $p < 0.05$.

We further characterized the hydrogel's swelling ratio which indicates water sorption capacity, thus predicting the rate of hydrogel degradation.[27] It was found that increasing GelMA concentrations from 5% to 20% resulted in reduced swelling ratios from 1500% to 500% ($p < 0.05$) (Figure 1E), likely due to increased crosslinking densities at 20% GelMA. This not

Table 1. Summary of physical properties of GelMA with different concentrations.

GelMA concentration [%]	Compressive modulus [kPa]	Tensile modulus [kPa]	Tensile strength [kPa]	Elongation at break [%]	Swelling ratio [%]	Degradation [%]		
						3 d	7 d	56 d
5	3 ± 1	9 ± 1	4 ± 1	40 ± 6	1476 ± 28	100	100	100
7.5	14 ± 2	17 ± 2	7 ± 1	39 ± 5	1273 ± 26	80 ± 5	100	100
10	26 ± 3	57 ± 9	18 ± 1	34 ± 5	719 ± 24	30 ± 2	65 ± 3	100
15	89 ± 9	153 ± 18	24 ± 2	27 ± 5	567 ± 19	20 ± 3	35 ± 4	100
20	108 ± 8	194 ± 16	29 ± 3	22 ± 4	470 ± 9	8±1	24 ± 4	80 ± 7

only limits the rate and amount of water penetration but is also thought to slow down degradation.[28]

To evaluate degradation, GelMA hydrogels were incubated in collagenase solution. As shown in Figure 1F,G, the degradation rate decreased with increasing GelMA concentrations, with complete degradation by less than 3 d (5% GelMA) to upward of 8 weeks (20% GelMA). Interestingly, 20% GelMA hydrogels remained present even after 8 weeks of incubation, albeit at significantly reduced size which may be attributable to increased methacrylamide crosslinks in 20% GelMA which are resistant to collagenase. Compared to previously developed collagen hydrogels which usually last for only 1 month,[16,17] GelMA hydrogels are thought to be better suited for long-term wound healing cases by remaining in the wound bed long term,[9] thus ensuring optimal healing whilst avoiding secondary infections.

The above results have suggested that the mechanical and degradation properties of GelMA hydrogels can be readily tuned to a great extent by varying GelMA concentrations. Compressive and elastic moduli could be tuned from a few kPa to a few hundred kPa, and the degradation times could be varied from a few days to several months (**Table 1**), indicating the hydrogel's broad spectrum of properties as skin substitutes in different body sites and for different wound types.

2.2. Cell Viability, Adhesion, and Proliferation on GelMA Hydrogels

2.2.1. Cell Viability

The ability of cells to attach, spread, and grow on hydrogels is of fundamental importance for tissue development.[29–33] We evaluated keratinocytes' viability by quantifying the live and dead cells adhered on the surfaces of hydrogels made from different concentrations of GelMA. Immortalized human keratinocytes (HaCaTs) were used in this study as an application of HaCaTs in epidermal tissue regeneration through cell culture, wound healing, and transplantation studies is well documented.[34–36] Cell viabilities were found higher than 90% at 1, 4, and 7 d for all GelMA concentrations (**Figure 2**A,C), demonstrating the innate biocompatibility of GelMA hydrogels.

2.2.2. Cell Adhesion and Proliferation

Investigation of the area of hydrogels covered by HaCaTs indicating cell attachment and the number of cells on the surfaces of GelMA over time indicating cell proliferation revealed that increasing the concentration of GelMA resulted in statistically significant increase in cellular attachment (Figure 2B,D, $p < 0.05$) and proliferation (Figure 2B,E, $p < 0.05$). This suggested that stiffer hydrogels and/or increased cell binding sequences arginylglycylaspartic acid (RGD) may promote cellular attachment on the hydrogels.[6] Overall, these results illustrated that HaCaT cells could proliferate on all GelMA hydrogels over a period of 7 d and that increasing the GelMA concentration could increase HaCaT attachment and proliferation.

Keratinocytes have to establish a confluent monolayer before developing a stratified epidermal layer.[37] On a macroscopic level, HaCaT cells were shown to proliferate and form a confluent layer after being submerged in culture media for 7 d or longer depending on GelMA concentrations, resulting in the formation of a transparent GelMA hydrogel (Figure S2A, Supporting Information), covered with a thin white cell sheet as shown in Figure S2B, Supporting Information. We further demonstrated that cells cultured on 20% GelMA hydrogels formed a confluent monolayer after 7 d of submerged culture as indicated by light microscopic images (see the example in Figure 2F-i) and presence of prominent fluorescence of E-cadherin (Figure 2F-ii), a cell-junction protein. The development of a confluent monolayer is vital for subsequent homogeneous epidermal stratification as nonuniform and patchy keratinocyte colony formation may result in some highly stratified areas sloughing off whilst other areas were only beginning to stratify.[38] As the 20% GelMA with increased methacrylamide crosslinks exhibited optimal compressive modulus (≈110 kPa) to support the keratinocyte adhesion and proliferation, these scaffolds were selected in the following study to reconstruct epidermis.

2.3. In Vitro Epidermal Development on GelMA Hydrogels

After a monolayer of HaCaT cells was developed, the constructs were lifted to air–liquid interface (ALI) to induce HaCaT differentiation and stratification. Macroscopically, lifting the construct to the ALI for 2 weeks resulted in the formation of a cell multilayer (Figure S2C, Supporting Information), which became thicker in week 6 under ALI conditions (Figure S2D, Supporting Information). Haematoxylin and eosin (H & E) stained images revealed that HaCaTs stratified and flattened on both GelMA (**Figure 3**A) and control collagen (Figure 3B) hydrogel surfaces after culture at ALI for 6 weeks.

Adv. Healthcare Mater. **2015**,
DOI: 10.1002/adhm.201500005

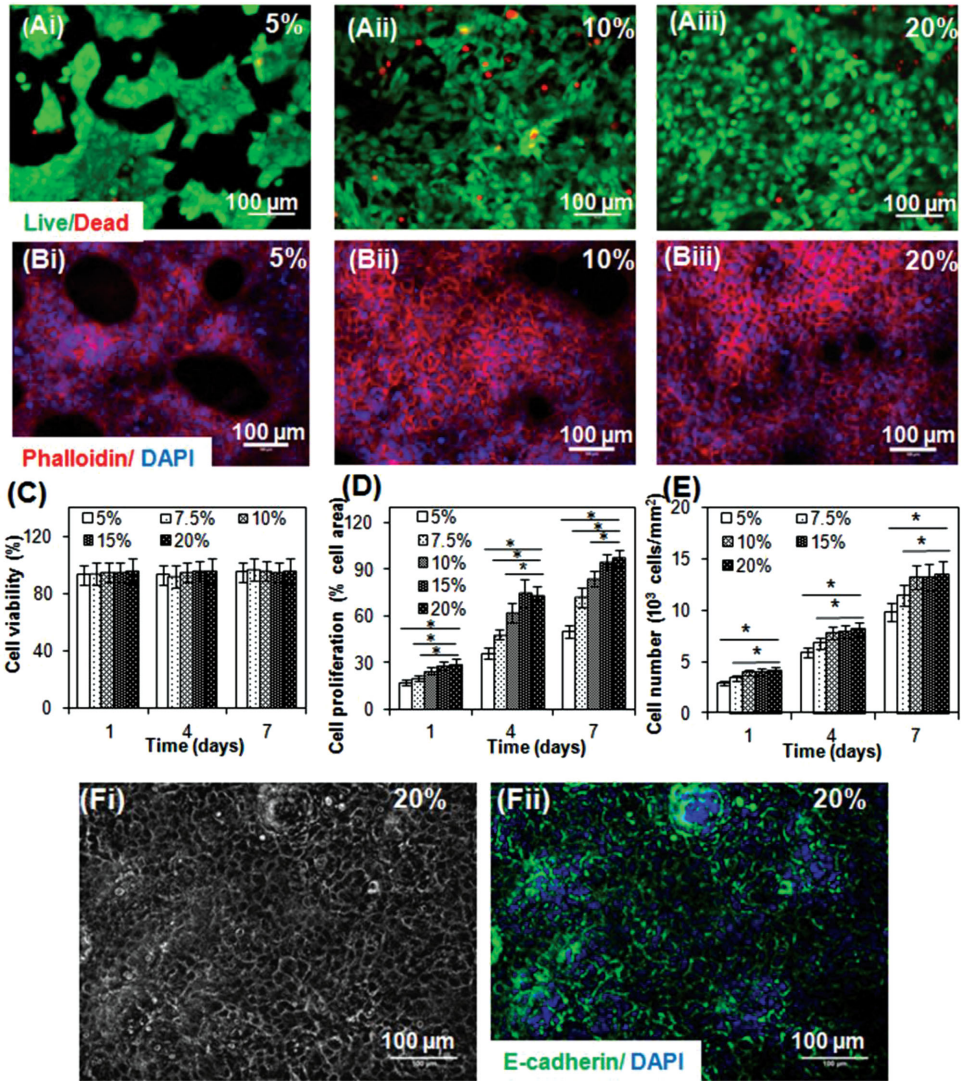

Figure 2. Viability, adhesion, and proliferation of HaCaT cells cultured on surfaces of GelMA with different concentrations. A) Representative live/dead fluorescence images of HaCaT cells on GelMA surfaces of 5% (i), 10% (ii), and 20% (iii) after 7 d of culture. Green fluorescent cells are alive and red fluorescent cells indicate dead cells. B) Representative phalloidin/DAPI fluorescence images of HaCaT cells on GelMA surfaces of 5% (i), 10% (ii), and 20% (iii) after 7 d of culture. Cell filaments are stained by phalloidin (red) and nuclei stained by DAPI (blue). C) Quantification of the staining using NIH ImageJ software of the live and dead cells of the 2D cultures of GelMA at different concentrations. D) Quantification of the staining using NIH ImageJ software of the sample area covered by cells of 2D cultures of GelMA with different concentrations. E) Quantification of the staining using NIH ImageJ software of the number of cells on surfaces of GelMA with different concentrations. * indicates $p < 0.05$. F) (i) is a representative phase contrast image of the cell monolayer developed on 20% GelMA after 7 d of culture and (ii) is the corresponding image of immunocytochemical staining of E-cadherin (green) in HaCaT cell junctions and DAPI nucleic staining (blue). Prominent fluorescence of E-cadherin in adjacent cells was observed.

Basal keratinocytes showed columnar morphology, whereas the keratinocytes further away from the constructs exhibited flattened morphology. With significant increase in thickness over time ($p < 0.05$), the developed epidermis was approximately 20, 50, and 100 µm after 2, 4, and 6 weeks, respectively, of ALI culture on both GelMA hydrogels and control collagen scaffolds (compare Figure 3A-i,ii, B–i,ii). There was no significant difference in thickness between the epidermis grown on GelMA or collagen ($p > 0.05$). The engineered epidermis on either scaffold was thinner compared to the sample of human abdomen epidermis (120 µm) (Figure 3C,D), but still within the range of native human epidermis (75–150 µm).[13] It is noteworthy that after 6 weeks of ALI culture, GelMA hydrogels were still present as opposed to collagen scaffolds which almost disappeared, indicating long-term substrate stability of the 20% GelMA hydrogels.

Protein expression analysis of the reconstructed epidermis on GelMA (**Figure 4**A) or control collagen (Figure 4B) hydrogels demonstrated the appearance of both ki67 (proliferation marker) and involucrin (terminal differentiation marker, expressed in the suprabasal layers of stratified squamous epithelium) after 6 weeks of ALI culture. The reconstructed epidermis exhibited slightly disorganized structure possibly due to the immature terminal differentiation of HaCaT cells[34,39] or to

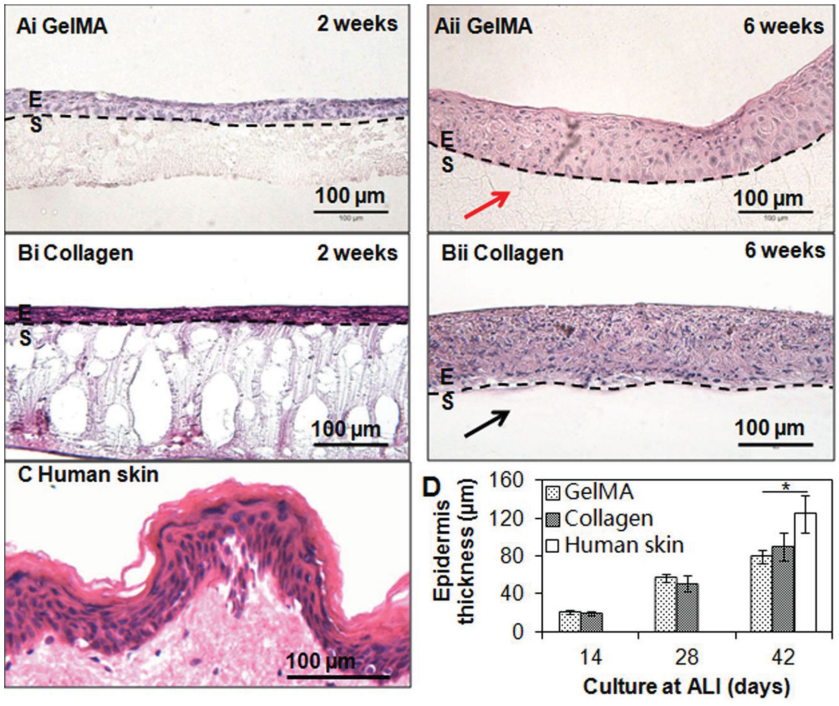

Figure 3. Reconstructed epidermis on hydrogel scaffolds. Examples of hematoxylin and eosin (H & E) stained sections of reconstructed epidermis on A) GelMA and B) control collagen scaffolds after 2 weeks (i) and 6 weeks (ii) of culture at air–liquid interface (ALI) and C) human epidermis. Flattening and stratification of HaCaT cells from the top surface of the reconstructed epidermis on either GelMA or collagen scaffolds can be clearly seen. Note the presence of GelMA (red arrow) and absence of collagen (black arrow) after 6 weeks of culture at ALI. Scale bar = 100 µm. D) Quantification of the thickness of the reconstructed epidermis at different times of culture at ALI and human epidermis. E = epidermis, S = scaffolds. * indicates $p < 0.05$.

the absence of paracrine signaling from fibroblasts during culture,[34–37,40] which may be normalized when cultured in vivo.[36] With significant increase over time, the developed epidermis had four, six, and ten layers after 2, 4, and 6 weeks, respectively, of ALI culture on either GelMA or collagen surfaces. Quantification of the layers of reconstructed epidermis showed no significant difference between the two substrates, and their thickness was comparable with the normal human epidermis consisting of 8–12 keratinocyte layers (Figure 4C,D).[41,42]

2.4. Barrier Formation of Reconstructed Epidermis

Electrical resistance measurements provide an indication of skin's barrier integrity and thus its relative hydration values.[43] Statistical analysis demonstrated significant differences between the relative resistances of collagen scaffolds, collagen scaffolds with reconstructed epidermis (epidermis (C)), GelMA hydrogels (20%), and GelMA hydrogels with reconstructed epidermis (epidermis (G)) ($p < 0.05$) (**Figure 5**A). Collagen scaffolds lacking an epidermis displayed least resistance at ≈700 Ω which had about half the value of the resistance of the corresponding GelMA hydrogels ($p < 0.05$). Barrier function of both scaffolds was predictably increased by the reconstructed epidermal layer compared to the cell-free substrates where the resistance of the epidermis (C) increased twofold from 700 to ≈1400 Ω (700 Ω increase) and that of epidermis (G) from 1700 to 2600 Ω (900 Ω increase) when compared to their cell-free equivalents. These results primarily indicated that the collagen scaffold had an inherently lower barrier integrity compared to GelMA hydrogels possibly due to high levels of crosslinking of the latter and lower water content,[44] and secondly that the addition of an epidermal layer successfully increased barrier properties probably due to functional tight junctions and a stratified architecture of confluent keratinocytes.[45,46] The resistance values of the reconstructed epidermis were smaller than that of human skin (1000–10 000 Ohm) possibly due to fewer degree of stratifications resulting from immature terminal differentiation of HaCaT cells[34,39] or absence of paracrine signaling from fibroblasts during culture,[34–37,39] which may be normalized when cultured in vivo.[41]

A tissue engineered skin substitute should ideally be able to control water loss from a wound bed[47] to prevent excessive dehydration, as well as the build-up of exudates.[48] As expected, scaffolds without an epidermal cover had significantly higher rates of water loss per day compared to those with an epidermis ($p < 0.05$) (Figure 5B). Collagen scaffolds had the lowest ability to retain water with loss rates approaching 3 g m^{-2} d^{-1} which was almost twice the amount lost by GelMA hydrogels, possibly due to the higher crosslinking density of GelMA which improved water retention. The addition of an epidermal layer significantly reduced water loss for both collagen and GelMA scaffolds with water loss rates being almost identical at around 1 g m^{-2} d^{-1}, less than the trans-epidermal water loss of normal human skin (≈4 g m^{-2} d^{-1}), possibly due to the lack of presence of sweat glands.[45] Interestingly, no difference could be observed between the collagen scaffolds layered with an epidermis and naked GelMA, indicative of a synergistic barrier function between GelMA hydrogels and the epidermis. These results indicated the significant protective barrier function for GelMA based reconstructed epidermis exerted by both the crosslinking and the epidermal cover. This is important as dehydration remains as one of the major complications of untreated severe skin losses due to extreme trans-epidermal water loss.[49,50]

Regenerated skin not only has to prevent loss of water from within the body but also functions as a relative barrier to harmful external insults. To evaluate the resistance of the reconstructed epidermis to external moisture, we studied the permeability of the scaffolds covered with epidermis and their cell-free counterparts to dextran solution. Dextran diffusion studies exhibited highest permeability at almost 100% for naked collagen scaffolds and lowest at 80% after 2 h of diffusion for epidermis (G) (Figure 5C). No difference was observed between epidermis (C) and the naked GelMA, corroborating the results obtained with water loss studies (see above). These

Adv. Healthcare Mater. 2015,
DOI: 10.1002/adhm.201500005

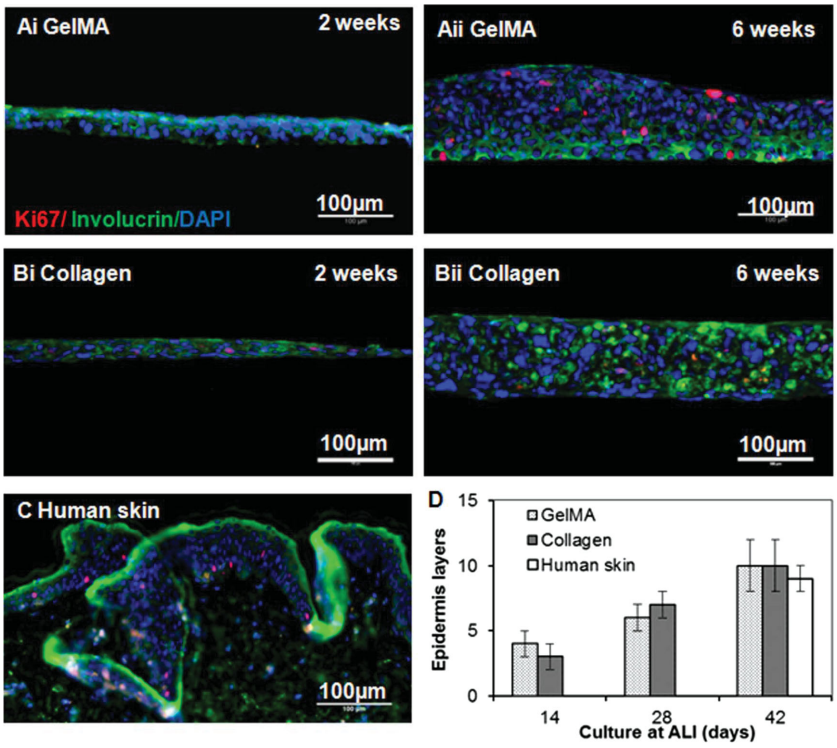

Figure 4. Expression of proteins of reconstructed epidermis on hydrogel scaffolds. Examples of ki 67 (red, proliferation maker), involucrin (green, differentiation marker), and DAPI (blue, nuclei) stained sections of reconstructed epidermis on A) GelMA and B) collagen scaffolds after 2 weeks (i) and 6 weeks (ii) of culture at ALI and C) human epidermis. Scale bar = 100 μm. D) Quantification of the number of epidermis layers of the reconstructed epidermis at different times of culture at ALI and human epidermis.

results, again, highlighted the importance of both the presence of crosslinked networks and the epidermal cover in preventing diffusion of water molecules either way across the skin. The above results have demonstrated that the reconstructed epidermis had increased resistance and decreased trans-epidermal water permeability, indicative of improved barrier functions.

Our work demonstrates a simple, cost-effective technique to reconstruct functional epidermis using a hydrogel based on photocrosslinkable GelMA with robust mechanical, degradation, and biological properties. These hydrogels were able to support the development of multilayered, renewable keratinocytes with similar organization and differentiation as human epidermis. Changes in GelMA concentration would provide the means to fine-tune its physical and biological properties in order to meet specific requirements as skin substitutes in different body sites and for different wound types.[51] Moreover, since GelMA is light-polymerizable, it could be easily molded or micropatterned into various shapes and configurations upon light exposure for a broad spectrum of tissue engineering applications.[22] In terms of skin regeneration, photocrosslinkable hydrogels may be particularly useful in the treatment of trauma wounds which are frequently extensive and irregular. Wound beds of any shape may easily and homogenously be filled using liquid uncrosslinked hydrogel precursors. Upon light exposure, photocrosslinking can thus enable solidification of the precursor. Alternatively, light-polymerizable GelMA could be applied to the regeneration of palmoplantar epidermis with ridges and the interphase between palmoplantar and normal hairy skin, where a gradient in epidermis thickness exists. Furthermore, the hydrogel nature endows GelMA with ready modification of its chemical and physical properties (e.g., incorporation or conjugation of different growth factors). The unique combination of photopolymerizability, optimal mechanical properties, biodegradability, and biocompatibility makes GelMA a promising material for skin tissue engineering.[22] Such an exceptional characteristic of GelMA also distinguishes it from other reported substrates to reconstruct epidermis including polycarbonate membrane[52] or decellularized porcine intestine[53] which cannot be tailor made according to the patient's own wounds and whose physical and chemical properties cannot be readily modified. We anticipate that the developed GelMA hydrogel could find applications as epidermal substitutes, wound dressings, or substrate to construct in vitro skin models. Future work will include the

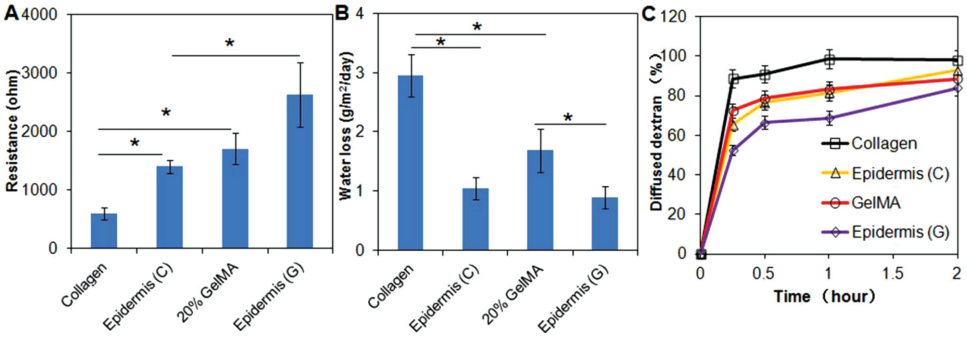

Figure 5. A) Resistance measurements, B) rate of water loss, and C) relative water permeability of naked collagen, collagen covered with a reconstructed epidermis (Epidermis (C)), GelMA hydrogel (20%), and GelMA hydrogel covered with epidermis (Epidermis (G)). Note the significant influence on barrier function of an epidermal cover. * indicates $p < 0.05$.

evaluation of fibroblasts within the dermal layer toward commercialization of this skin equivalent.

3. Conclusion

In this study, we have synthesized photocrosslinkable GelMA hydrogels with tunable mechanical and degradation features ideally suited as skin tissue engineering scaffolds. We have found that by varying the concentration of GelMA prepolymer solution, the physical and biological properties of the resultant hydrogels could be adequately controlled to meet the requirements for epidermis formation. Hydrogels of higher concentrations displayed improved material stiffness for cell adhesion and keratinocyte monolayer formation, combined with sufficiently prolonged resistance to collagenase degradation. GelMA hydrogels supported the formation of a stratified epidermis with a certain barrier function (e.g., electrical resistance and prevention of water loss). The authors envision that the developed GelMA hydrogels can find applications as epidermal substitutes, wound dressings, or substrates to construct in vitro skin models.

4. Experimental Section

Synthesis of GelMA: Synthesis of GelMA was described previously.[54] Briefly, 10.0 g of type A porcine skin gelatin (Sigma-Aldrich, St. Louis, MO) was added into 100 mL of Dulbecco's phosphate-buffered saline (DPBS) (Invitrogen, San Diego, CA) and dissolved by stirring at 60 °C using magnetic stirrer. 8.0 mL of methacrylic anhydride was then added to react with the gelatin solution under vigorous stirring for 3 h at 50 °C. Then, the reaction was stopped by a 5-fold dilution of the polymer solution with warm (40 °C) DPBS. Salts and unreacted methacrylic anhydride were removed from the mixture by 1 week dialysis with 12–14 kDa cut-off in distilled water at 40 °C. White porous foam was then obtained by lyophilizing the solution for 1 week and was stored at −80 °C until further use. The degree of methacrylamide modification was defined as the ratio of the number of methacrylamide groups tagged to gelatin to the number of amine groups in unreacted gelatin. Using ^{1}H NMR (Varian Inova 500), such value was obtained by the integration of peaks at 7.4 ppm corresponding to the aromatic residues of gelatin, and peaks at 5.5 ppm and 5.7 ppm corresponding to methacrylamide groups.[25]

Preparation of GelMA Hydrogels: Varying amounts of freeze-dried GelMA macromer were dissolved in DPBS containing 0.5% (w/v) 2-hydroxy-1-(4-(hydroxyethoxy)phenyl)-2-methyl-1-propanone (Irgacure 2959, CIBA Chemicals, Basel, Switzerland) as photoinitiator at 80 °C to make final GelMA concentrations at 5%, 7.5%, 10%, 15%, and 20% (w/v). The prepolymer solution was then pipetted into a polydimethylsiloxane (PDMS) mold, covered with 3-(Trimethoxysilyl) propyl methacrylate (TMSPMA)-treated glass slide and exposed to 6.9 mW cm^{-2} UV light (360–480 nm) for a certain period of time. For compression test, swelling ratio, and degradation study, samples of 6 mm diameter and 3 mm thickness were fabricated upon 180 s of UV exposures, whereas for tensile test, samples of 11 mm length, 5.5 mm width, and 1 mm thickness were fabricated using 60 s of UV exposures. For biological studies, samples of 6 mm diameter and 150 µm thickness were produced upon 20 s of UV exposure. The UV time for curing samples of different thicknesses was optimized to allow sufficient crosslinking of GelMA prepolymer solution of various concentrations. The sample thickness of 150 µm for biological studies was selected in present study to allow better epidermis reconstruction and easy handling. Preliminary results have shown that samples with thickness over 200 µm resulted in slightly disorganized multilayered epidermis (see Figure S3, Supporting Information), where the basal keratinocytes did not exhibit columnar morphology although the keratinocytes further away from the constructs exhibited flattened morphology. This may be due to the insufficient nutrient transport at ALI during culture. In addition, when the thickness of GelMA hydrogel was less than 100 µm, handling of the resultant hydrogel became difficult (e.g., placing the hydrogel on the cell inserts). For all tests, five replicates were used unless otherwise stated.

Characterization of Physical Properties of GelMA Hydrogels: A. Compression Test: Crosslinked samples were detached from the glass slide and incubated in DPBS at 37 °C for 24 h. The samples were then blotted dry and compressed at a rate of 1 mm min^{-1} using an Instron 5542 mechanical tester. The compressive modulus was calculated as the slope in the linear region of the stress–strain curve corresponding to 0%–10% strain.[55]

B. Tensile Test: Samples were incubated in DPBS at 37 °C for 24 h, and then blotted dry and fixed by two clamps of Instron 5542 mechanical tester. The samples were stretched at a constant rate of 1 mm min^{-1} at room temperature. The elastic modulus was determined as the slope in the linear region of the stress–strain curves corresponding to 0%–10% strain.[55]

C. Swelling Ratio Analysis: Samples were incubated in DPBS at 37 °C for 24 h, taken from DPBS, lightly blotted dry and weighed (W_S). Samples were then freeze-dried and weighed to determine the dry weight (W_D). The swelling ratio of the swollen gel (SR) was calculated according to Equation (1)[56]

$$SR = \frac{W_S - W_D}{W_D} \times 100\% \quad (1)$$

D. Degradation Study: Samples were placed in 1.5 mL Eppendorf tubes with 500 µL of DPBS with 2 U mL^{-1} of collagenase type II at 37 °C continuously for 3 weeks, then replaced with 500 µL of DPBS with 0.2 U mL^{-1} of collagenase for 5 weeks, which corresponds to the collagenase concentration during wound healing.[57] The collagenase solution was refreshed every 2–3 d to maintain constant enzyme activity. At predetermined time points, the collagenase solution was removed and the samples were washed with sterile deionized water two times, freeze-dried and weighed. Morphology of the samples at different time points was also recorded. The percentage degradation (D%) of the gels was determined using Equation (2)

$$D\% = \frac{W_0 - W_t}{W_0} \times 100\% \quad (2)$$

where W_0 is the initial sample dry weight and W_t is the dry weight after time t.

Development of HaCaT Monolayer: A. Culture of HaCaTs: HaCaTs were obtained from the German Cancer Research Center (DKFZ) (Heidelberg, Germany) and maintained as previously described.[58] Briefly, cells were cultured in Dulbecco's Modified Eagle's Medium (DMEM, Invitrogen, San Diego) supplemented with 10% fetal bovine serum (FBS) (Life Technologies, NY) and 1% penicillin/streptomycin (Life Technologies, NY) at 37 °C and 5% CO_2. Cells were maintained in tissue culture polystyrene and passaged at 1:6 when the cells reached 70% confluency.

B. Cell Viability: HaCaT cell suspension was seeded on the surface of samples with different GelMA concentrations at a seeding density of 5×10^4 cells cm^{-2}. A calcein AM/ethidium homodimer-1 live/dead assay (Life Technologies, NY) was performed according to the manufacturer's instructions to examine the cell viability on the GelMA hydrogels following 1, 4, and 7 d of culture in medium.[59] To stain the cells, medium was replaced with 300 µL of live/dead dye solution (0.5 µL of calcein AM and 2 µL of ethidium homodimer per 1 mL DPBS) for 15 min in the dark at 37 °C. The cells were then imaged using a Nikon Eclipse Ti-S fluorescence microscope. Total number of live and dead cells was quantified using NIH ImageJ software and the cell viability was determined as the ratio of live cells relative to the total cell number.

DOI: 10.1002/adhm.201500005

C. Cell Adhesion and Proliferation: Rhodamine-labeled phalloidin (Alexa Fluor 594, Life Technologies, NY) and DAPI (Sigma, St Louis, MO) were used for F-actin and cell nuclei staining, respectively, according to the manufacturer's instructions to examine cell adhesion on samples following 1, 4, and 7 d of culture in medium. Briefly, following 3× PBS wash, samples were fixed in 4% paraformaldehyde (PFA) for 30 min, permeabilized using 0.1% Triton X-100 for 20 min, and then blocked in 1% BSA for 45 min. Rhodamine-labeled phalloidin solution (dilution 1:40) was then added and incubated with the cells at 37 °C for 45 min. Finally, DAPI solution (dilution 1:1000) was added to the cells and incubated at 37 °C for 5 min. The cells were then imaged using Nikon fluorescence microscope, and the cell number and cell area were measured using NIH ImageJ software.[60]

D. Tight Junction Formation Analysis: To characterize the formation of a cell monolayer, after fixation, permeabilization, and blocking, the samples were stained with an E-Cadherin antibody (a cell adhesion molecule and epithelial cell marker) diluted 1:200 in PBS containing 1% BSA for 45 min at room temperature. Samples were subsequently incubated with FITC-labeled goat-anti-mouse secondary antibody (dilution 1:800, Life Technologies, NY) for 45 min in dark and then incubated with DAPI solution (dilution 1:1000) at 37 °C for 5 min. The cells were then imaged using Nikon fluorescence microscope, and the cell number and cell area were measured using NIH ImageJ software.

Reconstruction and Analysis of Epidermis: A. Epidermal Differentiation at ALI: To reconstruct epidermis, the hydrogel samples were placed into cell inserts with 6.5 mm diameter and 0.4 μm pore polycarbonate membrane (Corning Transwell-24 well permeable supports, Sigma-Aldrich, WI) and then seeded with HaCaTs at a density of 5×10^4 cells cm^{-2}. 1 mL of HaCaT growth medium was added to each well in order to get submerged culture condition. Medium was changed on a daily basis. Collagen hydrogels were fabricated according to manufacturer's instruction (Life Technologies, NY) and used as controls. Briefly, collagen (5 mg mL^{-1}), sterile 10X PBS, 1 mol L^{-1} NaOH, and sterile distilled water were mixed at the ratio of 8/1/0.2/0.8. 10 μL of the mixture was then added into the cell inserts and incubated at 37 °C for 40 min. The gels were rinsed by the cell culture medium prior to cell seeding. After 1 week of submerged culture, cells were lifted to ALI to induce differentiation. The differentiation medium used was DMEM/F12 (3:1, v/v) supplemented with 10% FBS, 1% penicillin/streptomycin, 1.8 mmol L^{-1} Ca^{2+}, 5 μg mL^{-1} insulin, 0.4 μg mL^{-1} hydrocortisone, 20^{-12} mol L^{-1} triiodothyronine, 0.18 mmol L^{-1} adenine, 5 μg mL^{-1} transferrin, 2 ng mL^{-1} transforming growth factor α (TGF-α), and 100 ng mL^{-1} granulocyte-macrophage colony-stimulating factor (GMCSF).[36,61,62] TGF-α and GMCSF were used to facilitate the formation of a stratified epithelium with more comparable structures to the cultures of primary human keratinocytes.[36] 360 μL of differentiation medium was used to maintain the ALI. Cells remained at the ALI for 6 weeks with regular changes of differentiation medium twice a day.

B. Histology Analysis: To view the stratified multilayer of resultant epidermal layer, samples (cultured at 2, 4, and 6 weeks after ALI) were fixed in 4% PFA for 30 min and washed 3× by DPBS. The samples were cryoprotected first in 15% sucrose solution for 4 h and then in 30% sucrose solution for another 4 h at room temperature. The fixed samples were then mounted using OCT compound (Fisher Scientific, MA) in Tissue-Tek Crymold (Sakura Finetek USA, Inc., Torrance, CA), frozen using a mixture of 100% ethanol and dry ice and stored at −80 °C prior to sectioning. Sections of 5 μm thickness were cut using a cryostat (Leica CM 3050; Leica Microsystems, Wetzlar, Germany) at −20 °C, collected on Superfrost microscope slides (Fisher Scientific, MA). Paraffin-embedded human abdominal skin excisions (from 39 year old female, Caucasian) were used as control in this study and were received from Drs. Chong-Hyun Won and Thanh-Nga Tran from the Cutaneous Biology Research Center at Massachusetts General Hospital under a protocol approved by the institutional review board.[58] The samples were cut at 5 μm using a Reichert-Jung 2035 microtome prior to staining with H&E. The section-mounted glass slides were immersed into a hematoxylin solution (Leica biosystems, IL) for 5 min, washed with tap water for 1 min, and dipped in 1% acid alcohol twice. It was further immersed in Bluing solution for 2 min and then in an eosin Y solution (Sigma Aldrich, WI) for 20 s. After washing with tap water for 1 min, the glass slides were sequentially immersed in a series of ethanol solutions (70%, 95%, 100% 2×), 2 min each for dehydration. After immersion in xylene for 3 min twice, the labeled glass slides were sealed with a coverslip using Permount Mounting Medium (Fisher Scientific, MA). Visualization of samples was performed using a Nikon microscope with infinicam.

C. Protein Expression of Developed Epidermis: Differentiation of HaCaTs was assessed by monitoring the expression of involucrin, (differentiation marker) and ki-67 (a proliferation marker). The sectioned samples were first permeabilized in 0.5% Triton X-100 for 5 min, then blocked twice using a mixture of 5% BSA and 10% goat serum for 30 min each. Samples were subsequently incubated with the primary antibodies to involucrin (Abcam, MA) at 1:100 for 45 min at room temperature and then with Alexa Fluor 488-conjugated secondary antibody (goat-anti-mouse antibody, dilution 1:500) (Life Technologies, CA) for 45 min in dark conditions at room temperature. Afterward, the samples were incubated with the primary antibodies to ki-67 (Abcam, MA) at 1:100 for 45 min and subsequently with Alexa Fluor 594-conjugated secondary antibody (goat-anti-rabbit antibody, dilution 1:800) (Life Technologies, CA) for another 45 min. Cell nuclei were then counter-stained with DAPI for 5 min. All samples were imaged immediately without mounting. Visualization of samples was performed using a Nikon Eclipse Ti-S fluorescence microscope. Prior to immunostaining, the control of sectioned paraffin-embedded human skin samples was antigen retrieved by boiling the samples in 10×10^{-3} M citrate buffer for 20 min at 120 °C and cooled for 30 min at room temperature.

D. Barrier Function of Reconstructed Epidermis: i. Trans-Epidermal Electrical Resistance: The electrical resistance of the reconstructed epidermis on hydrogels was directly measured using Agilent B2901A Precision Source/Measure Unit with 3 V direct current voltage loading.[38] Plain hydrogel scaffolds were used as control.

ii. Permeability of Reconstructed Epidermis: To examine the permeability of reconstructed epidermis, cell inserts with or without (control) samples were placed inside a just fit PDMS mold (9.5 mm diameter and 5 mm depth) containing 200 μL DPBS. 200 μL of 1.25 mg mL^{-1} fluorescence labeled dextran solution (Cascade Blue, 10 000 MW, Anionic, Lysine Fixable, Life Technologies, NY) was then added on top of the sample. The mold was incubated at 37 °C. At different time points (0.5, 1, and 2 h), 200 μL solution from the PDMS mold was transferred into a 96 well plate, and the quantity of dextran was measured using microplate reader (Bio-Tek, VT) at excitation wavelength of 360 nm and emission wavelength of 460 nm. Dextran standard curve was plotted as the fluorescence versus different dextran concentrations at 0.001, 0.01, 0.1, and 1 mg mL^{-1}. The percentage dextran permeability (P_{wp}) of the samples was determined using Equation (3)

$$P_{wp} = \frac{C_t}{\frac{M_0}{V_a + V_b}} \times 100\% \quad (3)$$

where C_t is the dextran concentration of samples calculated by a comparison with the standard curves. M_0 is the total amount of dextran used. V_a (i.e., 200 μL) and V_b (i.e., 200 μL) are the volumes of solution above and underneath the samples, respectively.

iii. Water Vapor Permeability of Reconstructed Epidermis: The water vapor permeability of the reconstructed epidermis on hydrogels was measured with the same setting used for dextran permeability measurement (cell inserts in PDMS mold). 200 μL of culture medium was added into the PDMS mold instead without the addition of medium on top of the sample. The mold was placed at 37 °C for 24 h. The weight of the mold before and after incubation was recorded to determine the water loss from the samples.[57]

Statistical Analysis: All data were expressed as mean ± standard deviation ($n = 3$). One-way ANOVA and Scheffe's post hoc test were used to determine statistical significance. $p < 0.05$ was considered significant.

Supporting Information

Supporting Information is available from the Wiley Online Library or from the author.

Acknowledgements

X.Z., Q.L., and L.Y. contributed equally to this work. The authors thank Dr. Chong-Hyun Won and Dr. Thanh-Nga Tran from Massachusetts General Hospital for the paraffin embedded human abdominal skin samples. The authors acknowledge funding from the National Science Foundation (EFRI-1240443), IMMODGEL (602694), and the National Institutes of Health (EB012597, AR057837, DE021468, HL099073, AI105024, AR063745).

Received: January 2, 2015
Revised: February 27, 2015
Published online:

[1] L. Braiman-Wiksman, I. Solomonik, R. Spira, T. Tennenbaum, *Toxicol. Pathol.* **2007**, *35*, 767.
[2] G. D. Winter, *Adv. Exp. Med. Biol.* **1977**, *94*, 673.
[3] J. K. Wagner, E. J. Parra, H. L. Norton, C. Jovel, M. D. Shriver, *Pigm. Cell Res.* **2002**, *15*, 385.
[4] R. V. Shevchenko, S. L. James, S. E. James, *J. R. Soc. Interface* **2010**, *7*, 229.
[5] S. MacNeil, *Nature* **2007**, *445*, 874.
[6] B. Trappmann, J. E. Gautrot, J. T. Connelly, D. G. Strange, Y. Li, M. L. Oyen, M. A. Cohen Stuart, V. Boehm Vogel, J. P. Spatz, F. M. Watt, W. T. Huck, *Nat. Mater.* **2012**, *11*, 642.
[7] J. E. Lee, J. C. Park, Y. S. Hwang, J. K. Kim, J. G. Kim, H. Sub, *Yonsei Med. J.* **2001**, *42*, 172.
[8] F. H. Silver, J. W. Freeman, D. DeVore, *Skin Res. Technol.* **2001**, *7*, 18.
[9] K. G. Harding, H. L. Morris, G. K. Patel, *BMJ* **2002**, *324*, 160.
[10] V. Keriquel, F. Guillemot, I. Arnault, B. Guillotin, S. Miraux, J. Amedee, J. C. Fricain, S. Catros, *Biofabrication* **2010**, *2*, 014101.
[11] J. L. Ifkovits, J. A. Burdick, *Tissue Eng.* **2007**, *13*, 2369.
[12] J. Zhu, R. E. Marchant, *Expert Rev. Med. Devices* **2011**, *8*, 607.
[13] E. De Vuyst, C. Charlier, S. Giltaire, V. De Glas, C. L. de Rouvroit, Y. Poumay, *Methods Mol. Biol.* **2014**, *1195*, 191.
[14] S. A. Oh, H. Y. Lee, J. H. Lee, T. H. Kim, J. H. Jang, H. W. Kim, I. Wall, *Tissue Eng. Pt. A* **2012**, *18*, 1087.
[15] L. Krishnan, J. A. Weiss, M. D. Wessman, J. B. Hoying, *Tissue Eng.* **2004**, *10*, 241.
[16] C. Helary, A. Abed, G. Mosser, L. Louedec, A. Meddahi-Pelle, M. M. Giraud-Guille, *J. Tissue Eng. Regen. M.* **2011**, *5*, 248.
[17] C. Helary, I. Bataille, A. Abed, C. Illoul, A. Anglo, L. Louedec, D. Letourneur, A. Meddahi-Pellé, M. M. Giraud-Guille, *Biomaterials* **2010**, *31*, 481.
[18] K. Hu, H. Shi, J. Zhu, D. Deng, G. Zhou, W. Zhang, Y. Cao, W. Liu, *Biomed. Microdevices* **2010**, *12*, 627.
[19] H. J. Levis, R. A. Brown, J. T. Daniels, *Biomaterials* **2010**, *31*, 7726.
[20] M. A. Awang, M. F. Abu Bakar, M. F. Mh Busra, S. Roy Chowdhury, N. F. Rajab, W. K. Wan Kamal, M. Y. Reusmaazran, M. Y. Aminuddin, B. H. Ruszymah, *Biomed. Mater. Eng.* **2014**, *24*, 1715.
[21] M. K. Yeh, Y. M. Liang, K. M. Cheng, N. T. Dai, C. C. Liu, J. J. Young, *Polymer* **2011**, *52*, 996.
[22] J. W. Nichol, S. T. Koshy, H. Bae, C. M. Hwang, S. Yamanlar, A. Khademhosseini, *Biomaterials* **2010**, *31*, 5536.
[23] C. S. Bahney, T. J. Lujan, C. W. Hsu, M. Bottlang, J. L. West, B. Johnstone, *Eur. Cells Mater.* **2011**, *22*, 43.
[24] Y. C. Chen, R. Z. Lin, H. Qi, Y. Yang, H. Bae, J. M. Melero-Martin, A. Khademhosseini, *Adv. Funct. Mater.* **2012**, *22*, 2027.
[25] H. Shin, B. D. Olsen, A. Khademhosseini, *Biomaterials* **2012**, *33*, 3143.
[26] J. Salber, S. Grater, M. Harwardt, M. Hofmann, D. Klee, J. Dujic, H. Jinghuan, J. Ding, S. Kippenberger, A. Bernd, J. Groll, J. P. Spatz, M. Möller, *Small* **2007**, *3*, 1023.
[27] M. B. Browning, S. N. Cereceres, P. T. Luong, E. M. Cosgriff-Hernandez, *J. Biomed. Mater. Res. A* **2014**, *102*, 4244.
[28] J. Lam, K. Kim, S. Lu, Y. Tabata, D. W. Scott, A. G. Mikos, F. K. Kasper, *J. Biomed. Mater. Res. A* **2014**, *102*, 3477.
[29] S. Bourdoulous, G. Orend, D. A. MacKenna, R. Pasqualini, E. Ruoslahti, *J. Cell Biol.* **1998**, *143*, 267.
[30] C. S. Chen, M. Mrksich, M. S. Huang, G. M. Whitesides, D. E. Ingber, *Science* **1997**, *276*, 1425.
[31] G. Davey, M. Buzzai, R. K. Assoian, *J. Cell Sci.* **1999**, *112*, 4663.
[32] A. Huttenlocher, M. H. Ginsberg, A. F. Horwitz, *J. Cell Biol.* **1996**, *134*, 1551.
[33] S. P. Palecek, J. C. Loftus, M. H. Ginsberg, D. A. Lauffenburger, A. F. Horwitz, *Nature* **1997**, *385*, 537.
[34] E. Boelsma, M. C. H. Verhoeven, M. Ponec, *J. Investig. Dermatol.* **1999**, *112*, 489.
[35] V. M. Schoop, N. Mirancea, N. E. Fusenig, *J. Investig. Dermatol.* **1999**, *112*, 343.
[36] N. Maas-Szabowski, A. Starker, N. E. Fusenig, *J. Cell Sci.* **2003**, *116*, 2937.
[37] J. G. Rheinwald, H. Green, *Cell* **1975**, *6*, 331.
[38] L. I. Bernstam, F. L. Vaughan, I. A. Bernstein, *In Vitro Cell Dev. B* **1986**, *22*, 695.
[39] M. Ponec, E. Boelsma, A. Weerheim, *Acta. Derm.-Venereol.* **2000**, *80*, 89.
[40] M. Peura, A. Siltanen, I. Saarinen, A. Soots, J. Bizik, J. Vuola, A. Harjula, E. Kankuri, *J. Biomed. Mater. Res. A* **2010**, *95*, 658.
[41] D. Breitkreutz, V. M. Schoop, N. Mirancea, M. Baur, H. J. Stark, N. E. Fusenig, *Eur. J. Cell Biol.* **1998**, *75*, 273.
[42] I. Brody, *J. Investig. Dermatol.* **1962**, *39*, 519.
[43] D. Y. Chau, C. Johnson, S. MacNeil, J. W. Haycock, A. M. Ghaemmaghami, *Biofabrication* **2013**, *5*, 035011.
[44] D. C. Fowles, R. E. Schneider, *Biol. Psychol.* **1974**, *2*, 67.
[45] P. van der Valk, C. K. van Kalken, H. Ketelaars, H. J. Broxterman, G. Scheffer, C. M. Kuiper, T. Tsuruo, J. Lankelma, C. J. Meijer, H. M. Pinedo, R. J. Scheper, *Ann. Oncol.* **1990**, *1*, 56.
[46] A. Narai, S. Arai, M. Shimizu, *Toxicol. In Vitro* **1997**, *11*, 347.
[47] R. K. Mishra, A. B. A. Majeed, A. K. Banthia, *Int. J. Plast. Technol.* **2011**, *15*, 82.
[48] B. Balakrishnan, M. Mohanty, P. R. Umashankar, A. Jayakrishnan, *Biomaterials* **2005**, *26*, 6335.
[49] A. B. Cua, K. P. Wilhelm, H. I. Maibach, *Br. J. Dermatol.* **1990**, *123*, 473.
[50] M. Fartasch, *Curr. Probl. Dermatol.* **1995**, *23*, 95.
[51] C. B. Hutson, J. W. Nichol, H. Aubin, H. Bae, S. Yamanlar, S. Al-Haque, S. T. Koshy, A. Khademhosseini, *Tissue Eng. Pt. A* **2011**, *17*, 1713.
[52] Y. Poumay, F. Dupont, S. Marcoux, M. Leclercq-Smekens, M. Herin, A. Coquette, *Arch. Dermatol. Res.* **2004**, *296*, 203.
[53] M. Jannasch, F. Groeber, N. W. Brattig, C. Unger, H. Walles, J. Hansmann, *Exp. Parasitol.* **2015**, *150*, 22.
[54] A. I. Van Den Bulcke, B. Bogdanov, N. De Rooze, E. H. Schacht, M. Cornelissen, H. Berghmans, *Biomacromolecules* **2000**, *1*, 31.
[55] W. Xiao, J. He, J. W. Nichol, L. Wang, C. B. Hutson, B. Wang, Y. Du, H. Fan, A. Khademhosseini, *Acta Biomater.* **2011**, *7*, 2384.
[56] L. Ferreira, M. M. Figueiredo, M. H. Gil, M. A. Ramos, *J. Biomed. Mater. Res. B Appl. Biomater.* **2006**, *77*, 55.
[57] M. S. Agren, C. J. Taplin, J. F. Woessner, W. H. Eagistein, P. M. Mertz, *J. Investig. Dermatol.* **1992**, *99*, 709.

[58] P. Boukamp, R. T. Petrussevska, D. Breitkreutz, J. Hornung, A. Markham, N. E. Fusenig, *J. Cell Biol.* **1988**, *106*, 761.
[59] H. Shin, B. D. Olsen, A. Khademhosseini, *Biomaterials* **2012**, *33*, 3143.
[60] J. Wu, X. Zhao, D. Wu, C.-C. Chu, *J. Mater. Chem. B* **2014**, *2*, 6660.
[61] I. Canton, D. M. Cole, E. H. Kemp, P. F. Watson, J. Chunthapong, A. J. Ryan, S. MacNeil, J. W. Haycock, *Biotechnol. Bioeng.* **2010**, *106*, 794.
[62] D. B. Haddow, R. M. France, R. D. Short, S. MacNeil, R. A. Dawson, G. J. Leggett, E. Cooper, *J. Biomed. Mater. Res.* **1999**, *47*, 379.